Fig S1

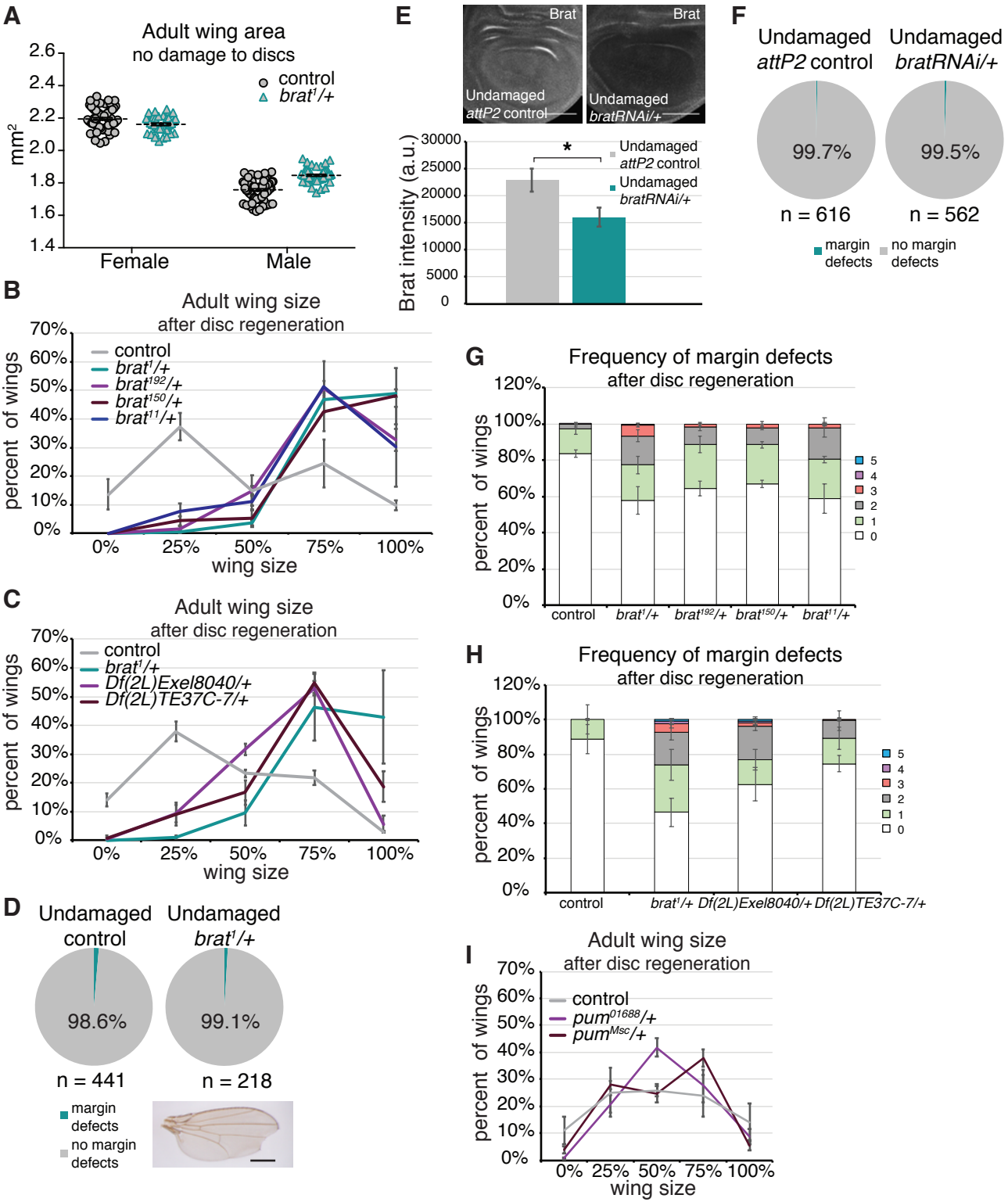
A
Adult wing area
no damage to discs
control
brat1/+
mm2
2.6
2.4
2.2
2.0
1.8
1.6
1.4
Female
Male
B
Adult wing size
after disc regeneration
control
brat1/+
brat192/+
brat150/+
brat11/+
percent of wings
70%
60%
50%
40%
30%
20%
10%
0%
0%
25%
50%
75%
100%
wing size
C
Adult wing size
after disc regeneration
control
brat1/+
Df(2L)Exel8040/+
Df(2L)TE37C-7/+
percent of wings
wing size
D
Undamaged
control
Undamaged
brat1/+
98.6%
99.1%
n = 441
n = 218
margin defects
no margin defects
E
Brat
Undamaged
attP2 control
Undamaged
bratRNAi/+
Brat intensity (a.u.)
30000
25000
20000
15000
10000
5000
0
*
F
Undamaged
attP2 control
Undamaged
bratRNAi/+
99.7%
99.5%
n = 616
n = 562
margin defects
no margin defects
G
Frequency of margin defects
after disc regeneration
percent of wings
120%
100%
80%
60%
40%
20%
0%
control
brat1/+
brat192/+
brat150/+
brat11/+
5
4
3
2
1
0
H
Frequency of margin defects
after disc regeneration
percent of wings
control
brat1/+
Df(2L)Exel8040/+
Df(2L)TE37C-7/+
I
Adult wing size
after disc regeneration
control
pum01688/+
pumMsc/+
percent of wings
0%
25%
50%
75%
100%
wing size

S1 Fig. Loss of *brat* does not cause enhanced growth or margin defects during normal development.

(A) Adult wing area measured using ImageJ after mounting and imaging wings, for undamaged control (w^{1118}) (n = 63 female and 70 male) and $brat^{1}$/+ (n = 38 female and 48 male) wings. *rnGAL4, GAL80^{ts}/TM6B* females were crossed to w^{1118} or $brat^{1}$/*SM6-TM6B* males and taken through the protocol shown in Fig 1A. (B) Adult wing sizes after disc regeneration for control (w^{1118}) (n = 599), $brat^{1}$/+ (n = 199), $brat^{192}$/+ (n = 237), $brat^{150}$/+ (n = 235) and $brat^{11}$/+ (n = 188) wings, from three independent experiments. (C) Adult wing sizes after disc regeneration for control (w^{1118}) (n = 396), $brat^{1}$/+ (n = 252), *Df(2L)Exel8040/*+ (n = 208) and *Df(2L)TE37C-7/*+ (n = 271) wings, from three independent experiments. (D) Margin defects detected in adult wings from undamaged control (w^{1118}) and $brat^{1}$/+ discs. *rnGAL4, GAL80^{ts}/TM6B* females were crossed to w^{1118} or $brat^{1}$/*SM6-TM6B* males and taken through the protocol shown in Fig 1A. Margin defects detected in the undamaged wings were never as severe as the ones seen in $brat^{1}$/+ wings after disc regeneration. A representative wing with margin defects is shown. (E) Anti-Brat immunostaining in undamaged control (*attP2*) and *bratRNAi/*+ discs. *rnGAL4, GAL80^{ts}/TM6B* females were crossed to *attP2* or *bratRNAi* males. Larvae were kept at 18°C and shifted to 30°C on day 7 AEL. Discs were dissected 24 hours after the shift to 30°C. Quantification of Brat fluorescence intensity in undamaged control *(attP2*) (n = 15) and *bratRNAi*/+ (n = 15) discs. Area for fluorescence intensity measurement was defined by wing pouch morphology and Anti-Myc co-immunostaining. * p = 0.02. (F) Margin defects detected in adult wings from undamaged control (*attP2*) and *bratRNAi* dics. *rnGAL4, GAL80^{ts}/TM6B* females were crossed to *attP2* or *bratRNAi*

males. Larvae were kept at 18°C and shifted to 30°C on day 7 AEL and kept there until eclosion. (G) Frequency of margin defects seen in adult wings after disc regeneration for control (w^{1118}) (n = 240), $brat^{1}$/+ (n = 191), $brat^{192}$/+ (n = 196), $brat^{150}$/+ (n = 213) and $brat^{11}$/+ (n = 152) wings. Wings in (G) are from the same experiments as (B). (H) Frequency of margin defects seen in adult wings after disc regeneration for control (w^{1118}) (n = 98), $brat^{1}$/+ (n = 223), *Df(2L)Exel8040/+* (n = 117) and *Df(2L)TE37C-7/+* (n = 194) wings. Wings in (H) are from the same experiments as (C). (I) Adult wing sizes after disc regeneration for control (w^{1118}) (n = 333), pum^{01688}/+ (n = 241) and pum^{Msc}/+ (n = 160) wings, from three independent experiments. Error bars represent SEM. Student's T-test used for statistical analyses. Scale bars are 100 μm.

Fig S2

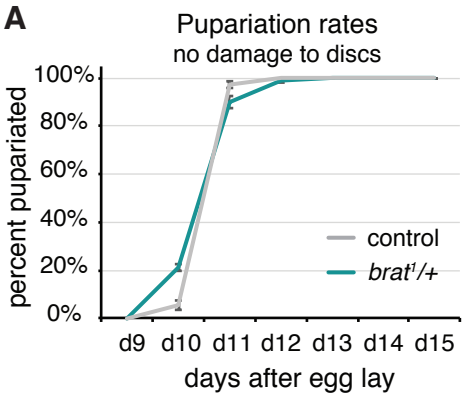
A
Pupariation rates
no damage to discs
percent pupariated
100%
80%
60%
40%
20%
0%
d9 d10 d11 d12 d13 d14 d15
days after egg lay
control
brat1/+

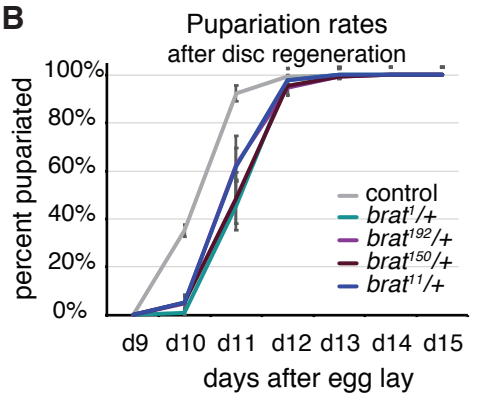
B
Pupariation rates
after disc regeneration
percent pupariated
100%
80%
60%
40%
20%
0%
d9 d10 d11 d12 d13 d14 d15
days after egg lay
control
brat1/+
brat192/+
brat150/+
brat11/+

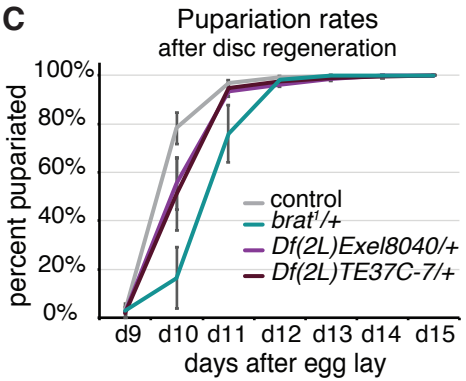
C
Pupariation rates
after disc regeneration
percent pupariated
100%
80%
60%
40%
20%
0%
d9 d10 d11 d12 d13 d14 d15
days after egg lay
control
brat1/+
Df(2L)Exel8040/+
Df(2L)TE37C-7/+

S2 Fig. Loss of *brat* delays pupariation in a regeneration-specific manner.

(A) Pupariation rates in undamaged control (w^{1118}) (n = 221) and $brat^{1}$/+ (n = 110) animals, from three independent experiments. (B) Pupariation rates after disc regeneration for control (w^{1118}) (n = 384), $brat^{1}$/+ (n = 107), $brat^{192}$/+ (n = 131), $brat^{150}$/+ (n = 114) and $brat^{11}$/+ (n = 113) animals. Pupariation rates are from the same experiments as in Fig 2A. (C) Pupariation rates after disc regeneration for control (w^{1118}) (n = 251), $brat^{1}$/+ (n = 146), *Df(2L)Exel8040/+* (n = 149) and *Df(2L)TE37C-7/+* (n = 162) animals, from three independent experiments. Error bars represent SEM.

Fig S3

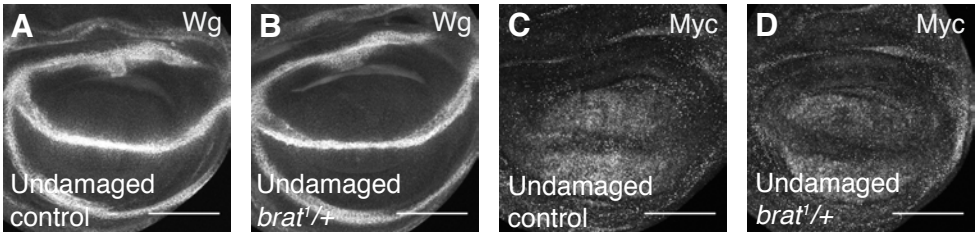
A
Wg
Undamaged
control
B
Wg
Undamaged
brat1/+
C
Myc
Undamaged
control
D
Myc
Undamaged
brat1/+

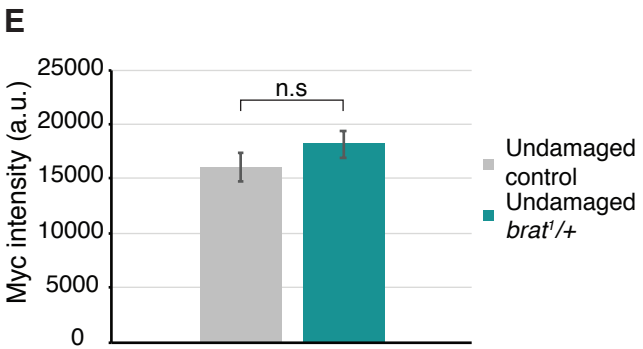
E
Myc intensity (a.u.)
25000
20000
15000
10000
5000
0
n.s
Undamaged
control
Undamaged
brat1/+

S3 Fig. Effects of loss of *brat* on Wg and Myc expression are regeneration-specific.

(A-B) Anti-Wg immunostaining in an undamaged control (w^{1118}) disc (A) and an undamaged $brat^{1}$/+ disc (B). (C-D) Anti-Myc immunostaining in an undamaged control (w^{1118}) disc (C) and an undamaged $brat^{1}$/+ disc (D). (E) Quantification of Myc fluorescence intensity in undamaged control (w^{1118}) (n = 10) and $brat^{1}$/+ (n = 10) discs. Area for fluorescence intensity measurement was defined by wing pouch morphology and the elevated Myc expression domain in the wing pouch. Error bars represent SEM. Student's T-test used for statistical analyses. Scale bars are 100 μm.

Fig S4

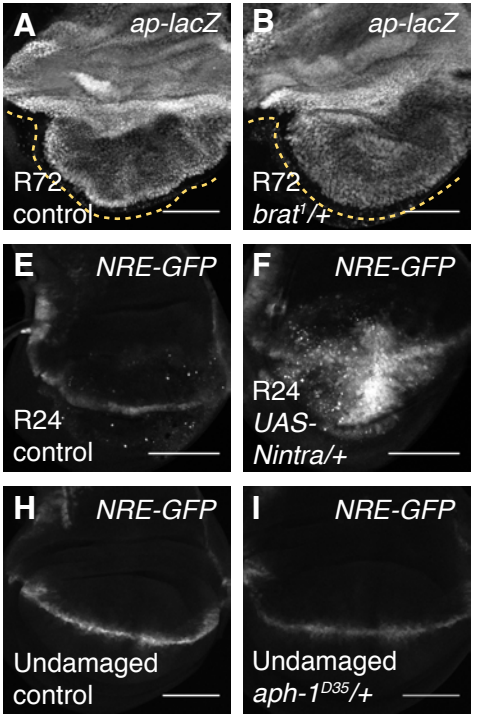
A
ap-lacZ
R72
control
B
ap-lacZ
R72
brat¹/+
E
NRE-GFP
R24
control
F
NRE-GFP
R24
UAS-
Nintra/+
H
NRE-GFP
Undamaged
control
I
NRE-GFP
Undamaged
aph-1D35/+

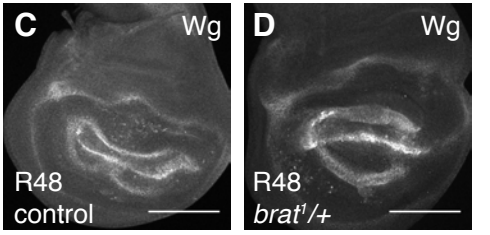
C
Wg
R48
control
D
Wg
R48
brat¹/+

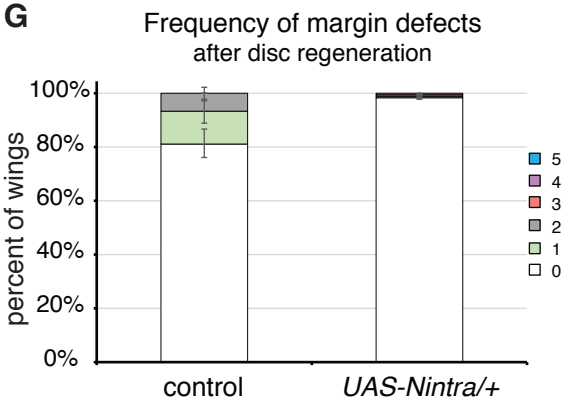
G
Frequency of margin defects
after disc regeneration
percent of wings
100%
80%
60%
40%
20%
0%
control
UAS-Nintra/+
5
4
3
2
1
0

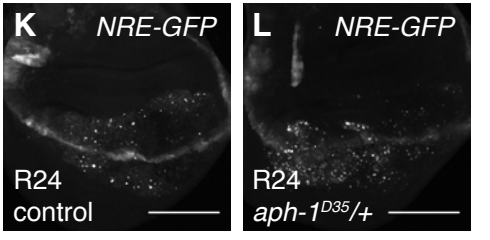
K
NRE-GFP
R24
control
L
NRE-GFP
R24
aph-1D35/+

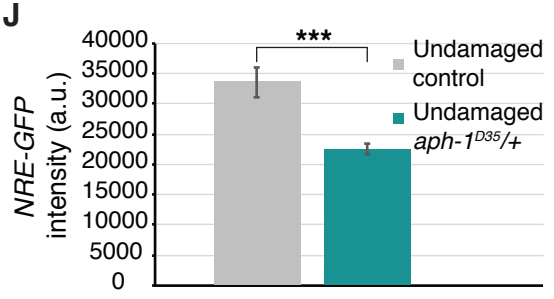
J
NRE-GFP
intensity (a.u.)
40000
35000
30000
25000
20000
15000
10000
5000
0
***
Undamaged
control
Undamaged
aph-1D35/+

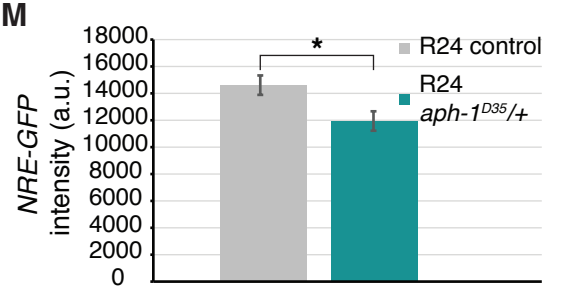
M
NRE-GFP
intensity (a.u.)
18000
16000
14000
12000
10000
8000
6000
4000
2000
0
*
R24 control
R24
aph-1D35/+

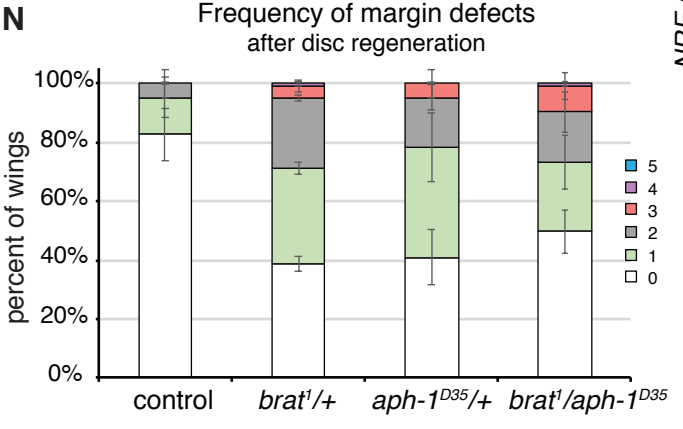
N
Frequency of margin defects
after disc regeneration
percent of wings
100%
80%
60%
40%
20%
0%
control
brat¹/+
aph-1D35/+
brat¹/aph-1D35
5
4
3
2
1
0

S4 Fig. Elevated Notch signaling does not cause margin defects.

(A-B) *ap-lacZ* expression in an R72 control (w^{1118}) disc (A) and an R72 $brat^{1}$/+ disc (B). Dashed yellow lines are drawn next to the DV boundary to highlight it. (C-D) Anti-Wg immunostaining in an R48 control (w^{1118}) disc (C) and an R48 $brat^{1}$/+ disc (D). (E-F) *NRE-GFP* expression in an R24 control (w^{1118}) disc (E) and an R24 *UAS-Nintra/+* disc (F). (G) Frequency of margin defects seen in adult wings after disc regeneration for control (w^{1118}) (n = 84) and *UAS-Nintra/+* (n = 357) wings, from five independent experiments. (H-I) *NRE-GFP* expression in an undamaged control (w^{1118}) disc (H) and an undamaged $aph\text{-}1^{D35}$/+ disc (I). *NRE-GFP*/+ and *NRE-GFP*/$aph\text{-}1^{D35}$ animals were raised at room temperature and dissected during third instar. (J) Quantification of GFP intensity in undamaged control (w^{1118}) (n = 15) and $aph\text{-}1^{D35}$/+ (n = 15) discs. *** $p < 0.0006$. (K-L) *NRE-GFP* expression in an R24 control (w^{1118}) disc (K) and an R24 $aph\text{-}1^{D35}$/+ disc (L). (M) Quantification of GFP intensity in R24 control (w^{1118}) (n = 13) and R24 $aph\text{-}1^{D35}$/+ (n = 11) discs. * $p < 0.02$. (N) Frequency of margin defects in adult wings after disc regeneration for control (w^{1118}) (n = 21), $brat^{1}$/+ (n = 137), $aph\text{-}1^{D35}$/+ (n = 38) and $brat^{1}/aph\text{-}1^{D35}$(n = 80) wings. Error bars represent SEM. Student's T-test used for statistical analyses. Scale bars are 100 μm.

Fig S5

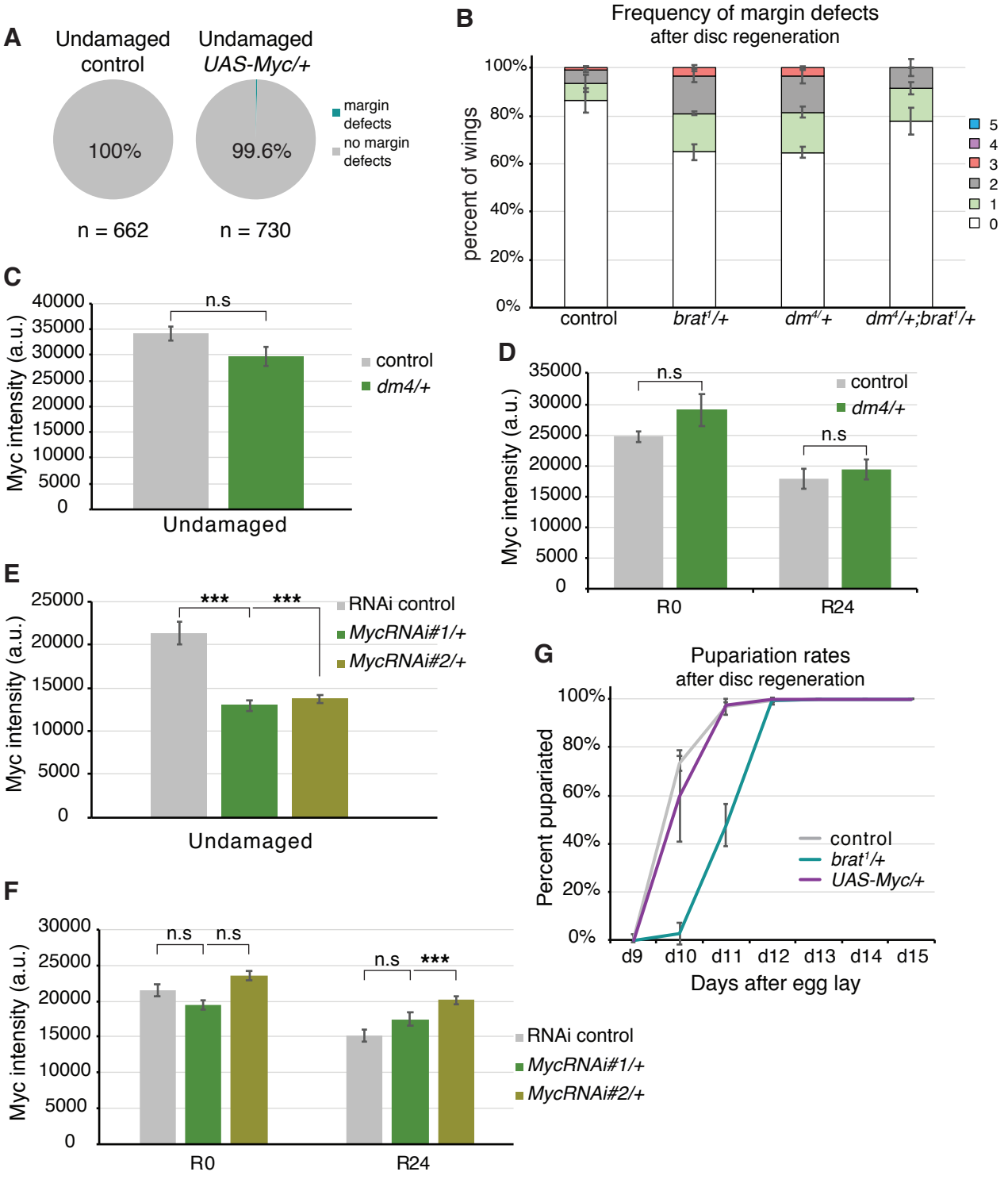
A
Undamaged control
Undamaged UAS-Myc/+
100%
99.6%
margin defects
no margin defects
n = 662
n = 730
B
Frequency of margin defects after disc regeneration
percent of wings
100%
80%
60%
40%
20%
0%
control
brat1/+
dm4/+
dm4/+;brat1/+
5
4
3
2
1
0
C
Myc intensity (a.u.)
40000
35000
30000
25000
20000
15000
10000
5000
0
n.s
control
dm4/+
Undamaged
D
Myc intensity (a.u.)
35000
30000
25000
20000
15000
10000
5000
0
n.s
n.s
control
dm4/+
R0
R24
E
Myc intensity (a.u.)
25000
20000
15000
10000
5000
0
***
***
RNAi control
MycRNAi#1/+
MycRNAi#2/+
Undamaged
F
Myc intensity (a.u.)
30000
25000
20000
15000
10000
5000
0
n.s
n.s
n.s
***
RNAi control
MycRNAi#1/+
MycRNAi#2/+
R0
R24
G
Pupariation rates after disc regeneration
Percent pupariated
100%
80%
60%
40%
20%
0%
control
brat1/+
UAS-Myc/+
d9
d10
d11
d12
d13
d14
d15
Days after egg lay

S5 Fig. Compensatory regulation prevents reduction of Myc expression during regeneration.

(A) Margin defects detected in adult wings from undamaged control (w^{1118}) and *UAS-Myc/+* discs. *rnGAL4, GAL80^{ts}/TM6B* females were crossed to w^{1118} or *UAS-Myc* males and taken through the protocol shown in Fig 1A. (B) Frequency of margin defects in adult wings after disc regeneration for control (w^{1118}) (n = 103), $brat^{1}$/+ (n = 203), dm^{4}/+ (n = 94) and dm^{4}/+; $brat^{1}$/+ (n = 94) wings, from three independent experiments. (C) Quantification of Myc fluorescence intensity in undamaged control (w^{1118}) (n = 12) and dm^{4}/+ (n = 11) discs. w^{1118} females were crossed to w^{1118} or *dm^{4}/FM7i, ActGFP* males and dissected when the animals were third instar. Area for fluorescence intensity measurement was defined by wing pouch morphology and the elevated Myc expression domain in the wing pouch. (D) Quantification of Myc fluorescence intensity in R0 control (w^{1118}) (n = 13), R0 dm^{4}/+ (n = 10), R24 control (w^{1118}) (n = 13), and R24 dm^{4}/+ (n = 10) discs. Area for fluorescence intensity measurement was defined by the elevated Myc expression domain in the wing pouch. (E) Quantification of Myc fluorescence intensity in undamaged control (VDRC genetic background line, called control) (n = 14), *MycRNAi#1/+* (n = 12), and *MycRNAi#2/+* (n = 13) discs. *rnGAL4, GAL80^{ts}/TM6B* females were crossed to the control, *MycRNAi#1*, or *MycRNAi#2* males. The animals were shifted to 30°C during early third instar and kept there for 28 hours then dissected. *MycRNAi#1/+* *** $p < 0.000007$, *MycRNAi#2/+* *** $p < 0.00002$. Area for fluorescence intensity measurement was defined by wing pouch morphology. (F) Quantification of Myc fluorescence intensity in R0 control (n = 13), R0 *MycRNAi#1/+* (n = 15), R0 *MycRNAi#2/+* (n = 13), R24 control (n = 13), R24 *MycRNAi#1/+* (n = 13), and R24

MycRNAi#2/+ (n = 13) discs. Fluorescence intensity was measured in the area marked by Anti-Nubbin immunostaining. *** $p < 0.00007$. (G) Pupariation rates after disc regeneration for control (w^{1118}) (n = 216), $brat^{1}$/+ (n = 114) and *UAS-Myc/+* (n = 209) animals, from three independent experiments. Error bars represent SEM. Student's T-test used for statistical analyses. Scale bars are 100 μm.

Fig S6

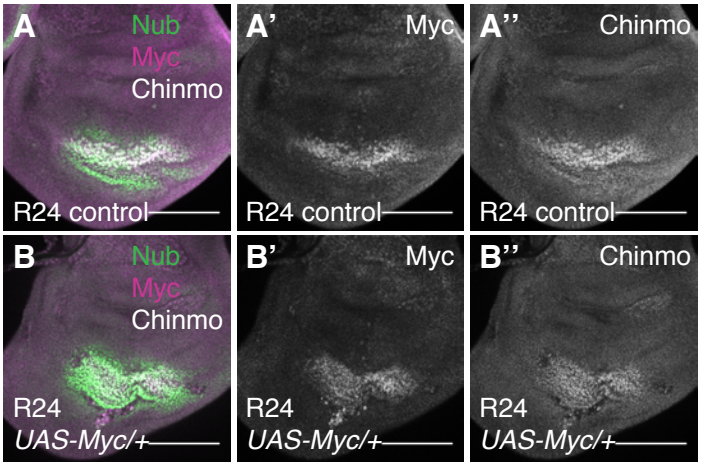
A
Nub
Myc
Chinmo
R24 control
A'
Myc
R24 control
A''
Chinmo
R24 control
B
Nub
Myc
Chinmo
R24
UAS-Myc/+
B'
Myc
R24
UAS-Myc/+
B''
Chinmo
R24
UAS-Myc/+

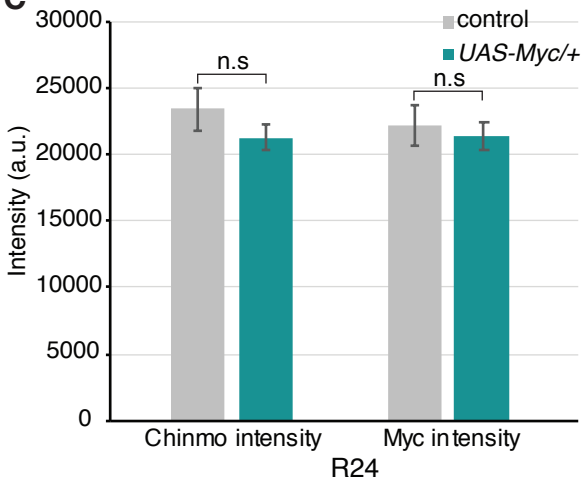
C
control
UAS-Myc/+
n.s
n.s
Intensity (a.u.)
30000
25000
20000
15000
10000
5000
0
Chinmo intensity
Myc intensity
R24

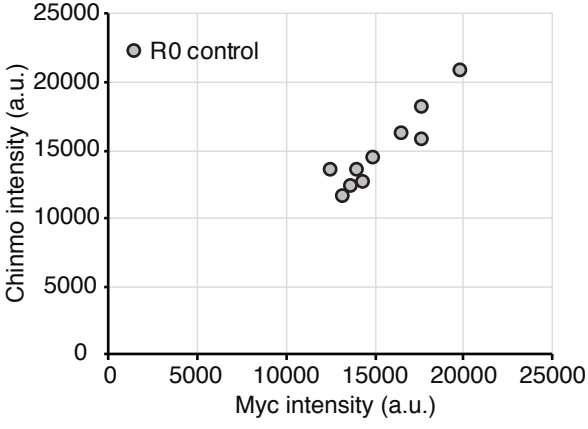
D
R0 control
Chinmo intensity (a.u.)
25000
20000
15000
10000
5000
0
0
5000
10000
15000
20000
25000
Myc intensity (a.u.)

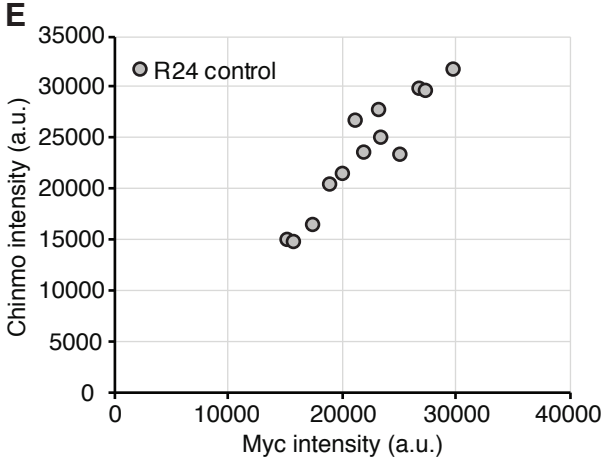
E
R24 control
Chinmo intensity (a.u.)
35000
30000
25000
20000
15000
10000
5000
0
0
10000
20000
30000
40000
Myc intensity (a.u.)

S6 Fig. Myc regulates Chinmo expression.

(A) Merge of anti-Nubbin, anti-Myc and anti-Chinmo immunostaining in an R24 control (w^{1118}) disc. (A'-A'') Same disc as (A) showing anti-Myc and anti-Chinmo immunostaining, respectively. (B) Merge of anti-Nubbin, anti-Myc and anti-Chinmo immunostaining in an R24 *UAS-Myc*/+ disc. (B'-B'') Same disc as (B) showing anti-Myc and anti-Chinmo immunostaining, respectively. (C) Quantification of Chinmo and Myc fluorescence intensity in R24 control (w^{1118}) (n = 13) and R24 *UAS-Myc*/+ (n = 14) discs. Area for fluorescence intensity measurement was defined by the elevated Myc expression domain in the wing pouch. Note that Myc and Chinmo expression co-localize. (D-E) Scatter plot showing correlation between Myc and Chinmo expression levels at R0 (D) and R24 (E). Pearson correlation coefficient for R0 = 0.93 and R24 = 0.94. Error bars represent SEM. Student's T-test used for statistical analyses. Scale bars are 100 μm.